Inelastic x-ray scattering study of the state-resolved differential cross section of Compton excitations in helium atoms

B. P. Xie,[1] L. F. Zhu,[2,*] K. Yang,[1,†] B. Zhou,[1] N. Hiraoka,[3] Y. Q. Cai,[3,‡] Y. Yao,[4] C. Q. Wu,[4] E. L. Wang,[2] and D. L. Feng[1,§]

[1]*Department of Physics, Surface Physics Laboratory (National Key Laboratory), and Advanced Materials Laboratory, Fudan University, Shanghai 200433, People's Republic of China*

[2]*Hefei National Laboratory for Physical Sciences at Microscale, Department of Modern Physics, University of Science and Technology of China, Hefei, Anhui 230026, People's Republic of China*

[3]*National Synchrotron Radiation Research Center, Hsinchu 30076, Taiwan, Republic of China*

[4]*Department of Physics, Fudan University, Shanghai 200433, Republic of China*

The state-resolved differential cross sections for both the $1s^2\ {}^1S_0 \to 1s2s\ {}^1S_0$ monopolar transition and the $1s^2\ {}^1S_0 \to 1s2p\ {}^1P_1$ dipolar transition of atomic helium had been measured over a large momentum transfer region by high-resolution inelastic x-ray scattering (IXS). The almost-perfect match of the present measurement with the theoretical calculations gives a stringent test of the theoretical method and the calculated wave functions. Our results demonstrate that high-resolution IXS is a powerful tool for studying the excitations in atoms and molecules.

After the discovery of the Compton effect in 1923, it was soon recognized that the Compton effect can give valuable information about the electronic momentum density of the target [1]. About 40 years later, Platzman and co-workers found that the Compton profile measured by the cross section of the Compton ionization gives information on the electron momentum distribution of the ground state. Furthermore, the Compton excitation measured through inelastic x-ray scattering (IXS) or x-ray Raman scattering can be used to probe the wave functions of electrons in an excited state [2]. The differential cross section (DCS) of the Compton excitation can be described by

$$\frac{d^2\sigma}{d\Omega d\omega_f} = r_0^2 \frac{\omega_f}{\omega_i} |\vec{\epsilon}_i \cdot \vec{\epsilon}_f^*|^2 S(\vec{q},\omega), \tag{1}$$

where $S(\vec{q},\omega)$ is the dynamical structure factor defined as

$$S(\vec{q},\omega) = \sum_f |\langle \psi_f | e^{-i\vec{q}\cdot\vec{r}} | \psi_i \rangle|^2 \delta(E_i - E_f + \hbar(\omega_i - \omega_f)), \tag{2}$$

$\omega = \omega_i - \omega_f$ is the energy loss, and $\vec{q} = \vec{k}_i - \vec{k}_f$ is the scattering vector. $S(\vec{q},\omega)$ provides a more comprehensive description of the excitations than the usual optical measurements, such as the photoabsorption, since it reveals the momentum distribution character related to the initial- and final-state wave functions ($|\psi_i\rangle$ and $|\psi_f\rangle$) [3]. The determination of the wave functions of a quantum many-body system, even as simple as a helium atom, is a challenging task, particularly for the excited states. Therefore, the study of the Compton

excitation would be important in building the fundamental pictures of quantum mechanics, atoms, molecules, and solids.

Although IXS has been known for over 40 years, this technique was mostly adopted to the study of condensed matter systems with high density, due to the very small cross section of the IXS [4,5]. For example, IXS has been proved successful in studying charge excitations of superconductors [6], graphite [7], ice [8], and organic molecular crystals [9]. The measurement of the Compton excitation on a low-density gas phase subject is hampered by the very weak signal that cannot fulfill the high-energy resolution requirement ($E/\Delta E \sim 10^5$) of the state-resolved measurement. In recent years, the advance of synchrotron techniques has enabled three pieces of investigation, to the best of our knowledge, on the Compton excitations in gases. Zitnik *et al.* reported the Compton excitation spectra near the xenon L_3 edge at a scattering angle of 90° with an energy resolution of 1 eV [10]. Kavcic *et al.* reported the spectra of argon gas, where the features related to different two-electron atomic processes near an inner-shell threshold are separated with an energy resolution of 0.6 eV [11]. Moreover, the Compton excitation spectra for the doubly excited states of helium at three angles were reported by Minzer *et al.* with an energy resolution of 0.9 eV [12]. However, the energy resolutions of 0.6–1 eV of these studies are not enough to resolve the adjacent transitions clearly, especially for the excitations of the valence shell state in atoms and molecules. Furthermore, there is so far no measurement of the DCS or dynamic structure factor $S(\vec{q},\omega)$ of the Compton excitation for a gas phase subject.

In an attempt to measure the state-resolved differential cross sections of the Compton excitation for gas phase, we investigated the $S(\vec{q},\omega)$ of the $1s^2\ {}^1S_0 \to 1s2s\ {}^1S_0$ and $1s^2\ {}^1S_0 \to 1s2p\ {}^1P_1$ transitions of atomic helium with ultrahigh-energy resolution and over a large momentum transfer region by IXS. The spectra had been measured with an energy resolution as high as 70 meV. The selection of helium is because it is the

---

*lfzhu@ustc.edu.cn

†Present address: Shanghai Institute of Applied Physics, Chinese Academy of Sciences, People's Republic of China.

‡Present address: NSLS-II, Brookhaven National Laboratory, USA.

§dlfeng@fudan.edu.cn

simplest multielectron system, for which a reliable theoretical calculation can be achieved. Therefore, the $S(\vec{q},\omega)$ measured with a high resolution would provide a benchmark to test the theoretical method stringently [13,14]. Historically, helium played an important role in the development of the Compton profile since a meaningful comparison between theory and experiment was feasible only on the helium atom at that time [15–17]. Furthermore, the DCSs for the $1s^2\,{}^1S_0 \rightarrow 1s2s\,{}^1S_0$ and $1s^2\,{}^1S_0 \rightarrow 1s2p\,{}^1P_1$ transitions have been studied by high-energy electron-energy-loss spectroscopy (EELS) [18,19], and the present measurement by IXS provides an independent cross-check.

The present IXS measurements were carried out at the Taiwan Beamline BL12XU of SPring-8 [5]. Helium gas (3 atm) was sealed in a gas cell with Kapton windows [Fig. 1(a)]. The energy spread of the incoming beam depends on the monochromator. Two energy resolution setups were exploited. A Si(333) high-resolution monochromator or a Si(400) monochromator was in place to achieve the resolution of 70 or 170 meV, respectively. Si(555) spherical analyzers with a 2-m radius of curvature were used to collect the scattered photons. The analyzer energy for the scattered photon was fixed at 9889.68 eV, while the incident photon energy varied, from which the energy loss is deduced. The momentum resolution is about 0.17 Å^{-1} (or 0.091 a.u. in atomic units). The total absorption of the x ray is about 13%, which mostly comes from the Kapton window and is constant in the scanned energy range. The scattering signal from the Kapton window

is far from the center of the gas cell, and is mostly blocked by the postsample slit. It does contribute to a tiny constant background at the small 2θ angle region, which can be easily removed during data analysis. The incident beam spot is about 80×120 μm^2. All the data were taken at room temperature. As illustrated in Fig. 1(b), the different lengths of the scattering pathway would be detected with varying 2θ, because of the finite size of the gas cell. This leads to an angular factor of $\sin(2\theta)$, which needs to be corrected to extract the DCS of the Compton excitation. The fluctuation of the incident x-ray intensity is monitored through a silicon *p-i-n* diode and can be corrected accordingly.

Selected IXS spectra of helium are shown in Fig. 2(a) with the assignments for the transitions based on the energy positions of the NIST database [20], and one of the spectra at momentum transfer $q^2 = 1.89$ a.u. fitted with multiple Gaussian peaks with full width at half maximum (FWHM) of 70 meV is illustrated in Fig. 2(b), for example. Different from the photoabsorption dominated by the dipolar transition, the IXS can excite not only dipolar transitions but also transitions of other multipolarities [2,3,21]. As a result, the excitations from the $1s^2\,{}^1S_0 \rightarrow 1s3s\,{}^1S_0$ monopolar transition to the $1s^2\,{}^1S_0 \rightarrow 1s3p\,{}^1P_1$ dipolar transition are clearly resolved at the present energy resolution of 70 meV, which is the best energy resolution achieved to our knowledge for the gas target of IXS and even slightly better than 80 meV of the high-energy EELS [18,22]. The measured peak width is limited by the energy resolution as illustrated in Fig. 2(b). It can also be seen from Fig. 2(a) that the monopolar transition is much weaker than the dipolar transition at the low-momentum transfer region, while the situation is reversed at the high-momentum transfer region. This illustrates that the dipole approximation for the IXS cross sections breaks down in the high-momentum transfer region [23]. This was reported previously in lithium metal [24], but the current results give a more direct example of this important aspect of the IXS, as calculation is not necessary here to identify the types of the transitions. A similar situation has been observed in high-energy EELS experiments before [25].

To determine the DCSs of the $1s^2\,{}^1S_0 \rightarrow 1s2s\,{}^1S_0$ and $1s^2\,{}^1S_0 \rightarrow 1s2p\,{}^1P_1$ excitations, their respective scattered photon intensities at the energy loss positions of 20.616 and 21.218 eV were measured by scanning the scattering angle 2θ from $5°$ to $60°$. To calibrate the background, a 2θ scan was run at 20.1-eV energy loss, since it is in a flat and featureless region of the IXS spectrum (Fig. 2). After correcting the contribution of background and effective scattering volume at different scattering angles [Fig. 1(b)], the dynamic structure factors $S(\vec{q},\omega)$ for these two transitions were obtained via dividing the DCSs by the factor of $\cos^2(2\theta)\omega_f/\omega_i$ for the incident photon polarization in the scattering plane, and scaling the value of the $1s^2\,{}^1S_0 \rightarrow 1s2p\,{}^1P_1$ transition to the theoretical one at $q^2 = 0.81$ a.u. Figure 3 shows the measured dynamic structure factors $S(\vec{q},\omega)$ of the monopolar excitation of $1s^2\,{}^1S_0 \rightarrow 1s2s\,{}^1S_0$ and the dipolar one of $1s^2\,{}^1S_0 \rightarrow 1s2p\,{}^1P_1$ along with some previous high-energy EELS data [18,19]. Theoretical calculations based on the explicitly correlated wave functions are also presented [14]. Compared with the commonly used Hylleraas-type wave functions, Cann and Thakkar used the exponential correlation factors to describe
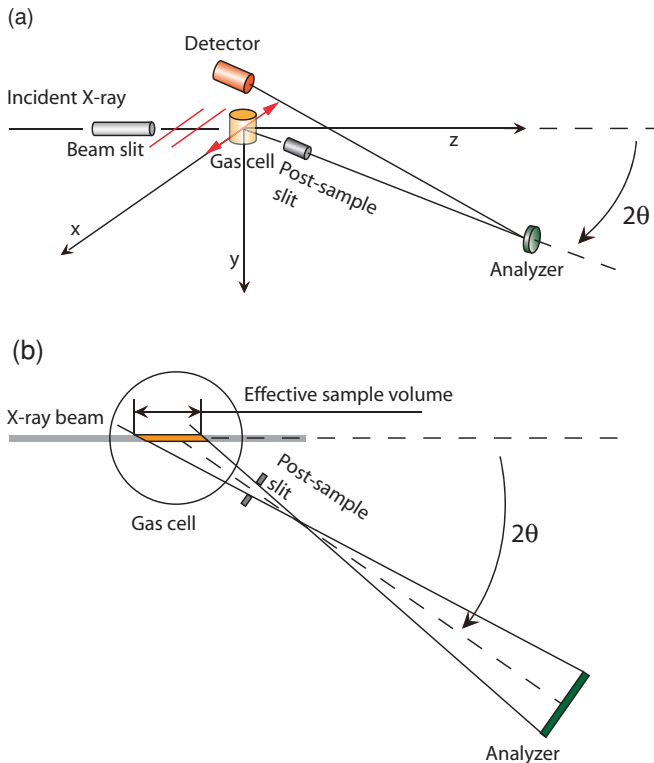

(a)

FIG. 1. (Color online) (a) Schematics of the experimental setup for the inelastic x-ray scattering of gases. The polarization direction of the incident photon is along the *x* axis. (b) Deduction of the effective sample volume (top view).
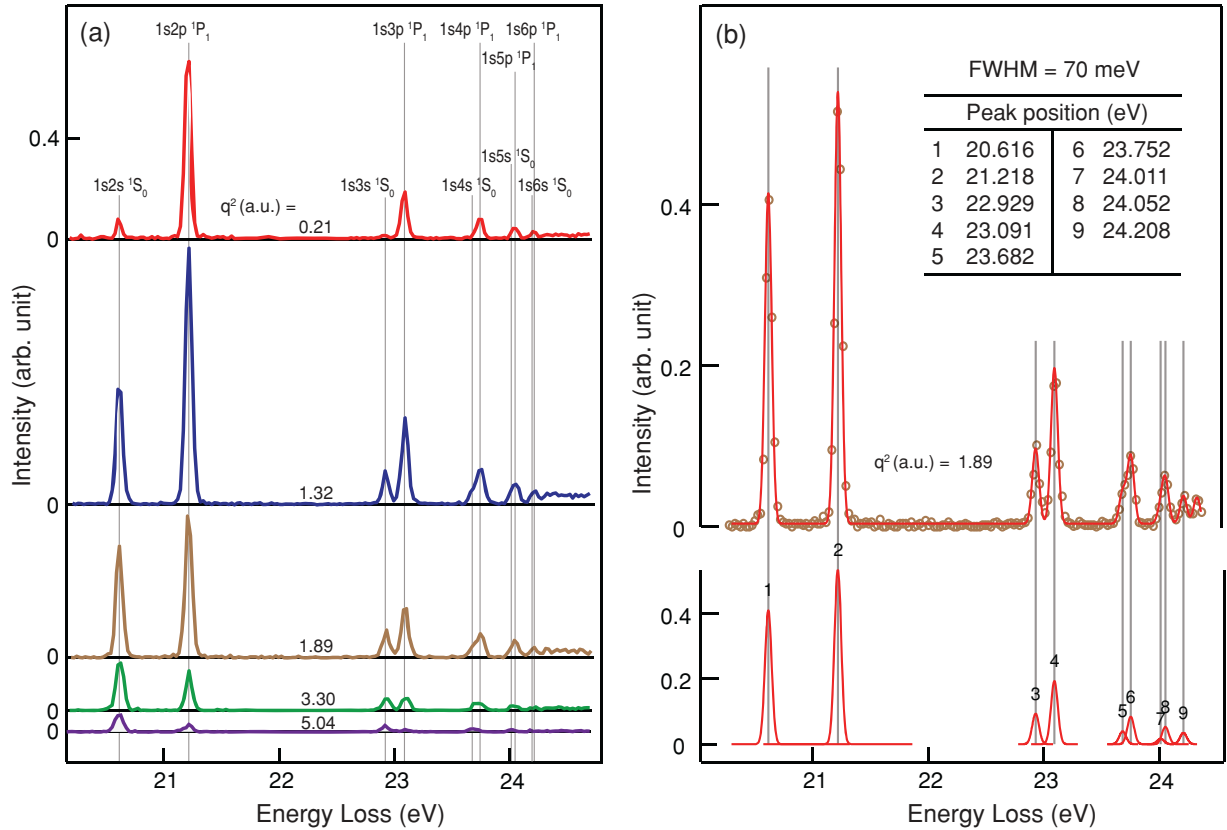
FIG. 2. (Color online) (a) Inelastic x-ray scattering spectra of helium gas as a function of energy loss at different momentum transfers with a resolution of 70 meV; the peaks are labeled by the final-state configurations excited from the $1s^2\ ^1S_0$ ground state. One of the spectra fitted with multiple Gaussian peaks with FWHM of 70 meV is illustrated in (b); the open circles indicate the experimental data while the solid lines are the fitted result.

the electron correlations in their calculation, and the calculated energies are in agreement with the best published values within nanohartrees [14]. Figure 3 illustrates the almost-perfect match of the theoretical curves with the present data over a broader momentum range, proving that the calculated wave functions are close to the actual wave functions to a great detail in the real space. As an experimental signature of the fact that the wave function of $1s2p\ ^1P_1$ is more extended in real space than that of $1s2s\ ^1S_0$, the $S(\vec{q},\omega)$ for the dipolar excitation is concentrated in the low-momentum transfer region, while that for the monopolar excitation is much broader in momentum space.

It is worth noting that the IXS and high-energy EELS are complementary. Measuring $S(\vec{q},\omega)$ by these two independent techniques provides an important means of data cross-check [12]. The extraction of $S(\vec{q},\omega)$ from high-energy EELS data is based on the validity of the first Born approximation (FBA), which requires a high incident electron energy [21]. As for how high the incident energy has to be, it can only be determined on a trial-and-error basis. The situation is more serious for the multielectron atoms or molecules, where the validity of the FBA has not been tested even now in EELS. However, the IXS is more straightforward [2], so that its cross section can serve as a benchmark to test whether the FBA holds in EELS experiments as well as the calculated wave

functions. Then, using the wave functions tested by the IXS data, only one key problem (i.e., the theoretical description of the interaction between the incident electron and atom or molecule) is left for the collision process at low or moderate kinematic energies, which will purify the theoretical problem and help to advance atomic and molecular theory. Moreover, high-energy EELS has much larger cross sections than IXS for the lower momentum transfer. However, this cross-section advantage of the electron scattering method rapidly diminishes with a rate of q^{-4} (Rutherford cross section) as the momentum transfer increases, while the cross section of the Compton scattering is simply proportional to $S(\vec{q},\omega)$. It is also known that high-energy EELS suffers from multiple scattering at high q, while the IXS does not. Generally speaking, high-energy EELS is more effective to study the large-scale structures of wave functions (lower q), while IXS is reliable at all length scales. As a result, the collection of IXS data presented in Fig. 3 over such a broad momentum range only takes several hours, while high-energy EELS data requires several weeks. Since the pressure in the gas cell could be further increased, there is a tremendous potential for the IXS in studying the excitations of atoms and molecules.

Practically, the IXS technique could be readily extended to more applied research where the gas systems may be subject to various extreme physical and chemical conditions, such
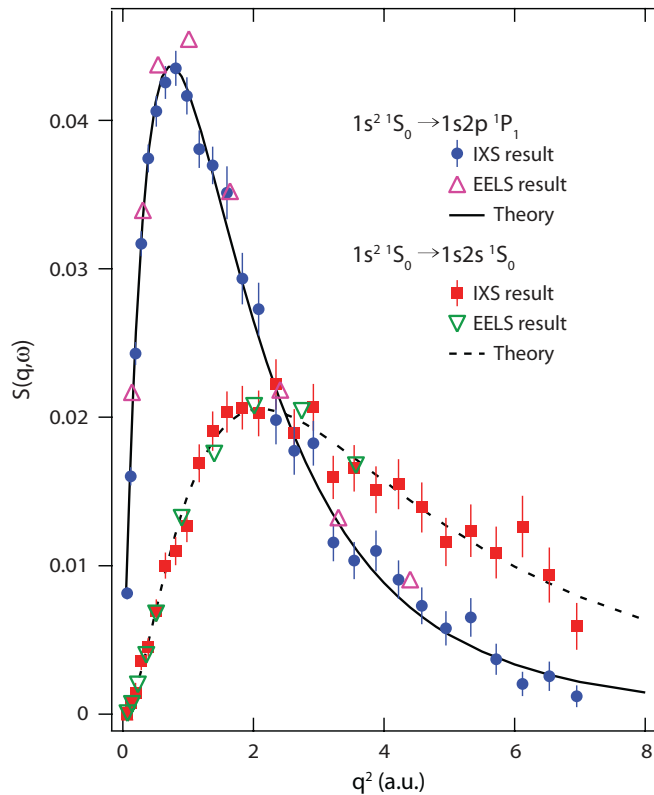
FIG. 3. (Color online) The dynamic structure factor $S(\vec{q},\omega)$ of the $1s^2\ {}^1S_0 \rightarrow 1s2s\ {}^1S_0$ monopolar transition and the $1s^2\ {}^1S_0 \rightarrow 1s2p\ {}^1P_1$ dipolar transition of helium measured by IXS. The high-energy EELS data [18,19] and the theoretical calculations [14] were converted from the generalized oscillator strengths. Data were taken with 170-meV resolution. Note the horizontal axis is $q^2 = k_i^2 + k_f^2 - 2k_i k_f \cos(2\theta)$, following the convention in atomic physics.

as in catalysis, or under extreme pressure and temperature conditions. These experimental environments are beyond the reach of other experimental techniques such as EELS and photoemission.

In conclusion, we have demonstrated that IXS is a powerful tool to study the excitations in atomic or molecular systems at a third-generation synchrotron. The dynamic structure factors of the $1s^2\ {}^1S_0 \rightarrow 1s2s\ {}^1S_0$ monopolar excitation and the $1s^2\ {}^1S_0 \rightarrow 1s2p\ {}^1P_1$ dipolar excitation of atomic helium have been measured by high-resolution IXS over a wide momentum transfer range. The almost-perfect match of the present measurement with the theoretical calculations gives a rigorous test of the theoretical method, and demonstrates the cleanliness of the data. Furthermore, our data provide a benchmark for the direct determination of the absolute DCS values of other gases in future experiments (e.g., with a mixed-gas setup).

[1] J. W. M. Du Mond, Phys. Rev. **33**, 643 (1929); Rev. Mod. Phys. **5**, 1 (1933).

[2] P. M. Platzman and N. Tzoar, Phys. Rev. **139**, A410 (1965); P. Eisenberger and P. M. Platzman, Phys. Rev. A **2**, 415 (1970).

[3] M. Y. Amusia, L. V. Chernysheva, Z. Felfli, and A. Z. Msezane, Phys. Rev. A **65**, 062705 (2002).

[4] W. Schülke, *Electron Dynamics by Inelastic X-Ray Scattering* (Oxford Science Publications, Oxford, 2007).

[5] Y. Q. Cai *et al.*, in *Synchrotron Radiation Instrumentation: Eighth International Conference on Synchrotron Radiation Instrumentation*, AIP Conf. Proc. No. 705 (AIP, New York, 2004), p. 340 and references therein.

[6] Y. Q. Cai *et al.*, Phys. Rev. Lett. **97**, 176402 (2006).

[7] W. L. Mao *et al.*, Science **302**, 425 (2003).

[8] Y. Q. Cai *et al.*, Phys. Rev. Lett. **94**, 025502 (2005).

[9] K. Yang *et al.*, Phys. Rev. Lett. **98**, 036404 (2007).

[10] M. Zitnik, M. Kavcic, K. Bučar, A. Mihelic, M. Stuhec, J. Kokalj, and J. Szlachetko, Phys. Rev. A **76**, 032506 (2007).

[11] M. Kavcic, M. Zitnik, K. Bucar, A. Mihelic, M. Stuhec, J. Szlachetko, W. Cao, R. AlonsoMori, and P. Glatzel, Phys. Rev. Lett. **102**, 143001 (2009).

[12] M. Minzer, J. A. Bradley, R. Musgrave *et al.*, Rev. Sci. Instrum. **79**, 086101 (2008).

[13] X. Y. Han and J. M. Li, Phys. Rev. A **74**, 062711 (2006).

[14] N. M. Cann and A. J. Thakkar, J. Electron Spectrosc. Relat. Phenom. **123**, 143 (2002).

[15] P. Eisenberger, Phys. Rev. A **2**, 1678 (1970).

[16] P. Eisenberger and W. A. Read, Phys. Rev. A **5**, 2085 (1972).

[17] H. F. Wellenstein and R. A. Bonham, Phys. Rev. A **7**, 1568 (1973).

[18] X. J. Liu, L. F. Zhu, Z. S. Yuan *et al.*, J. Electron Spectrosc. Relat. Phenom. **135**, 15 (2004).

[19] K. Z. Xu, R. F. Feng, S. L. Wu, Q. Ji, X. J. Zhang, Z. P. Zhong, and Y. Zheng, Phys. Rev. A **53**, 3081 (1996).

[20] The energy levels of helium can be found on the web site of NIST, [http://www.nist.gov/PhysRefData/ASD/].

[21] M. Inokuti, Rev. Mod. Phys. **43**, 297 (1971).

[22] X. J. Liu, L. F. Zhu, Z. S. Yuan, W. B. Li, H. D. Cheng, Y. P. Huang, Z. P. Zhong, K. Z. Xu, and J. M. Li, Phys. Rev. Lett. **91**, 193203 (2003).

[23] W. Schülke, J. Phys.: Condens. Matter **13**, 7557 (2001).

[24] M. H. Krisch, F. Sette, C. Masciovecchio, and R. Verbeni, Phys. Rev. Lett. **78**, 2843 (1997).

[25] W. F. Chan, G. Cooper, and C. E. Brion, Phys. Rev. A **44**, 186 (1991).

[26] J. A. Bradley, G. T. Seidler, G. Cooper, M. Vos, A. P. Hitchcock, A. P. Sorini, C. Schlimmer, and K. P. Nagle, Phys. Rev. Lett. **105**, 053202 (2010).